US - Ukraine Workshop on Innovative Combustion and Aerothermal Technologies in Energy and Power Systems
Kiev, Ukraine (May 21-24, 2001)

LASER DIAGNOSTIC MEASUREMENTS IN A LEAN-PREMIXED LABORATORY-SCALE GAS TURBINE COMBUSTOR

Thomas H. Fletcher
Paul O. Hedman

Chemical Engineering Department
Brigham Young University
Provo, Utah 84602

ABSTRACT

Significant progress has been made in computational fluid dynamic (CFD) modeling of gas turbine systems, particularly in the compressor and turbine regions. Models of the combustor section are not used with the same degree of confidence. One of the major reasons for the lack of confidence in the combustor models is the lack of data for evaluation, especially at high pressure. Detailed profile data obtained in an atmospheric laboratory-scale premixed combustor are now available for four swirling lean premixed conditions. Laser-Doppler anemometry (LDA) was used to measure velocities, planar laser-induced fluorescence (PLIF) was used to monitor OH and CH, and coherent anti-Stokes Raman spectroscopy (CARS) was used to measure temperature and major species concentrations. All of these techniques generated multiple points, so that both mean values and probability density functions are available at each location. The Reynolds' stresses <u'v'> are also available in both mean and PDF form. These data provide a good means to evaluate current CFD combustion models. In the future, we hope to be able to obtain similar data at high pressure.

INTRODUCTION

Background. This study was part of a U.S. Department of Energy's Advanced Turbine Systems (ATS) program to develop and commercialize ultra-high efficiency, environmentally superior, and cost competitive gas turbine systems for base-load applications in the utility, independent power producers, and industrial markets.

The LSGTC simulates many of the key combustor characteristics of commercial gas turbines. The use of advanced optical diagnostics permits near-instantaneous, non-intrusive measurement of such quantities as velocity (LDA), temperature (CARS), flame shape (PLIF), and species concentrations (PLIF and CARS) that are essential for model validation. LDA measurements have been made in clean combustion environments. The CARS instrument has been used in many different flames ranging from clean, laminar, premixed flames to particle-laden (pulverized coal), highly turbulent, diffusion flames. PLIF has recently been used to obtain instantaneous two-dimensional images of OH and CH radicals in a turbulent, swirling, premixed natural gas/air flame. The data also give insight into the physical processes governing the operation of practical gas turbine combustors. This insight has provided considerable direction to the modeling of the combustion process, and a database suitable for model subcode evaluation and verification.

In addition to the experimental work performed under this contract, other funding also supported research at BYU on advanced gas turbine models. A list of publications is available on the web (www.et.byu.edu /~tom/gas_turbines/Relevant_Publications.html)

Objectives. The objective of the study was to modify the existing laboratory scale gas turbine combustor (LSGTC) and use three laser diagnostic instruments (PLIF, LDA, and CARS) to make instantaneous in situ measurements with in the flame zone of the swirl stabilized combustor. The instantaneous in situ measurements provide insight into the combustion characteristics of the burner, and also provide a set of data for model verification and comparison. Past experience at BYU/ACERC has shown that the modeling of combustion behavior is more accurate and proceeds more rapidly when coupled with pertinent, foundational experimental research. Also, comparisons of model predictions to actual data are necessary to validate the accuracy of the code predictions.

Approach. A 2-dimensional, laboratory-scale combustor was designed to "specifically reproduce recirculation patterns and LBO processes that occur in a real gas turbine combustor" (Sturgess, et al., 1992). The combustor was designed to closely model the flow and combustion processes that occur in a real gas turbine combustor, but in a simpler, near 2-dimensional axisymmetric geometry. The model combustor was also designed with optical access so laser-based diagnostic instruments could be used to measure the various combustion and flow field characteristics associated with the combustion. The laser-based diagnostics used

in the program included: 1) two-component laser Doppler anemometry (LDA) to obtain gas velocity; 2) coherent anti-Stokes Raman spectroscopy (CARS) to obtain gas temperature and limited species concentrations; and 3) planar laser induced fluorescence (PLIF) to obtain 2-D images of OH and CH combustion intermediates. All of the laser instruments provided sets of multiple instantaneous measurements that could be interpreted in terms of mean and standard deviation properties. The local probability density functions (PDF) at up to 200 local ***in situ*** locations in the flame zone of the combustor were obtained for all three types of measurements. In addition to the specific ***in situ*** measurements mentioned, film and video cameras were used to examine flame structure and flame stability.

There were four separate experimental test conditions examined during the course of this study. Complete data sets from measurements of PLIF, LDA, and CARS were obtained at medium and high swirl levels for two lean premixed natural gas stoichiometric ratios (φ= 0.65 and φ= 0.80). The high swirl case at φ= 0.80 was the most stable flame condition tested. The medium swirl case at φ= 0.65 was very near the lean flammability limit for this burner, and consequently was very unstable. Example experimental results from the most stable case (HS, φ= 0.80) and the least stable case (MS, φ= 0.65) are included in the following sections of this paper. Some comparisons to model predictions are also included.

EXPERIMENTAL APPARATUS

Swirl is often used in a gas turbine combustor to stabilize the flame. Figure 1 presents an illustration of the flow vortex that results from such stabilization. The premixed fuel is rotated rapidly as it is passed through the swirl injector. This swirling flow field creates a strong central vortex, and at least 2 major recirculation zones, a central recirculation zone, a side recirculation zone. The central recirculation zone causes a reversal in the flow velocity in the center part of the combustor, which provides a stagnation region that can stabilize the flame. The bluff body of the combustor creates a slide recirculation zone with rotation between the walls of the combustor and bluff base. Depending on the level of swirl and the stoichiometry of the flame, one or another of these recirculation zones will provide the major source of flame stabilization.

An atmospheric pressure laboratory-scale model of a gas turbine combustor (LSGTC) was provided to this laboratory by Wright-Patterson Air Force Base (Roquemore, 1992) as part of an Air Force study on the combustion characteristics of a practical Pratt & Whitney injector in a atmospheric pressure model gas turbine combustor. Extensive CARS gas temperature measurements and LDA velocity measurements were obtained in the LSGTC with various practical, non-premixed injectors of particular interest to researchers at Wright-Patterson Air Force Base and Pratt & Whitney Aircraft Co. (Hedman, et al., 1995, Hedman and Warren, 1995, and Warren and Hedman, 1997).

This test facility was modified for use in this program to include a pressurized natural gas feed system and a generic turbulent, swirling premixed natural gas/air injector. Figure 2 shows a schematic of the combustor. The air and fuel are premixed externally to the combustion chamber and the mixture is fed into the fuel tube. Uniform mixing of gaseous fuel and air is assured by: 1) the length of the tube from the mixing point to the burner, and 2) by the sonic disrupter that was used in a previous program to control combustion instability. The sonic disrupter is a small cone with many small holes in its conical surface. The premixed fuel/air flows through the cone from the outside, forming a number of jets that impinge in the center of the cone. The impinging jets ensure that the fuel/air feed is completely mixed.

The air supply system provides air flows up to 4000 slpm. An airflow rate of 500 slpm was used throughout this study. This flow rate was sufficient to get reasonable combustion simulation but simplified the operation of the facility.

A natural gas compressor was used to pressurize a manifold of conventional gas cylinders up to a pressure of 2000 psia. The pressure from this blow-down natural gas system was reduced with pressure regulators, and the flow rate was controlled with a simple needle valve. Flow rates were measured with a rotameter. Flow rates of natural gas were adjusted to give the appropriate fuel equivalence ratio for the particular test condition of interest.

The LSGTC provided by Wright-Patterson Air Force Base was modified to incorporate the generic turbulent, swirling, premixed natural gas/air injector of this study. The central fuel tube from the original design was used to feed the fuel/air mixture to the burner. The new burner design was configured to easily integrate into the existing combustion chamber and to take advantage of fuel/air feed systems that were already in place.

The new premixed burner, shown schematically in Figure 3, was designed to connect directly to the existing fuel tube. Provision was made to prevent flame flashback into the premixed fuel tube by installing a brass flame arrester. The flame arrester is a block of solid brass that was drilled in a hexagonal pattern with sixty separate, 0.120 inch diameter holes. The high gas velocity (at least 19 m/s) through these holes

ensures that the flame can not propagate back into the feed tube.

Since the flames of interest in this study were to simulate those of a swirl stabilized practical gas turbine combustor; provision was also made in the injector to swirl the premixed flow. This was done by installing a cylindrical brass swirl block where eight rectangular slots of 0.125 inch width were machined at a prescribed angle. Three different swirl blocks were fabricated where the angles from the vertical were 30, 45, and 60 degrees. The three swirl blocks give theoretical swirl numbers (Beér and Chigier, 1972) of 0.43 (LS), 0.74(MS), and 1.29(HS). For this study, only medium swirl (MS), and high swirl (HS) injectors were used.

PLANAR LASER-INDUCED FLUORESCENCE (PLIF) MEASUREMENTS OF OH

Planar laser-induced fluorescence (PLIF) is a valuable tool for studying combustion phenomena. Flame propagation is partly governed by the diffusion and transport of important combustion intermediates like OH. Laser-induced fluorescence has the potential of measuring trace amounts of these short-lived combustion species at near instantaneous temporal resolution (10 ns). Likewise, because PLIF is laser-based, probing of the burner is non-intrusive. Laser-induced fluorescence measurements are often made at the focal point of a converging excitation laser. However, fluorescence can also be captured instantaneously over a two-dimensional area. The two-dimensional area captured resembles an instantaneous photograph-like image of the concentration of the combustion species being probed using a thin sheet of laser light tuned to the appropriate wavelength. The PLIF images provide near instantaneous images of the turbulent flame structure, including information regarding the location of flame fronts and size of turbulent eddies. This information is very useful in analyzing burner designs, understanding combustion phenomena, and validating combustion computer models.

Details of the PLIF instrument have been reported previously (Hedman, et al., 1998). For this study, an excitation wavelength of ca 283 nm was used for the OH radical. The 283 nm UV laser light was generated by frequency doubling 566 nm laser light from a tunable dye laser (Spectra Physics PDL-3) with a KD*P crystal in the wave extender (WEX). The tunable dye laser used a Nd:Yag laser as a pump source. The 10 ns UV laser beam from the WEX was directed to the LSGTC and formed into a thin two-dimensional sheet of laser light about 0.5 mm thick and ca 100 mm in width. The fluorescence images of the OH radical at ca 308 nm was captured on an electronic camera that uses an intensified charge coupled display (ICCD) with an electronic shutter speed of 100 ns. The ICCD camera was setup orthogonal to the 2-D laser sheet and was fitted with an appropriate filter (to block unwanted light) and a Nikon quartz f/1.2 lens. Two hundred fifty six separate “instantaneous” PLIF images were captured for each of the four test conditions and saved to the computer for later data analysis.

Figure 4 presents four example instantaneous images for each of the four test conditions. There are four images presented for each test condition. Those identified with the letter A represent the minimum intensity image collected. Those identified with the letter B represent a near average intensity image. Those identified with the letter C represent the maximum intensity image collected. Those identified with the letter D were included because of the oddity of the image collected. The numbers associated with each image are just the sequential numbers in the set of 256 images. The capture of each image was sufficiently separated so that there was no stochastic information available from image to image. However the set of 256 images has been analyzed to determine mean and standard deviation at each pixel in the image. The software used to generate the image normalizes the image to the maximum pixel count (red). Consequently, red in one image corresponds to a different pixel count than red in another image. The actual pixel counts are available, and have been used to provide PDFs of the pixel count distribution at given locations within the flame. LIF theory indicates that the pixel count is proportional to the actual concentration of OH. Unfortunately, calibration of the pixel counts into actual concentrations was beyond the scope of this study.

The stochastic nature of the flame is readily apparent from the images presented. The effect of swirl and fuel equivalence ratio on flame structure and stability are readily apparent. The OH images flames at high swirl show increased stability and more intense images at both high and low fuel equivalence ratios. The images at medium swirl and $\varphi = 0.80$ are also intense and stable. The flame at medium swirl and $\varphi = 0.65$ was very unstable, and was near lean blowout. In fact the flame at these operating conditions would occasional extinguish for no apparent reason.

The collection of 256 separate images for each test condition have been used to determine pixel by pixel mean and standard deviation images for each of the four test conditions. Figure 5 presents examples of the mean PLIF OH images for the HS, $\varphi = 0.80$ (most stable flame), and MS, $\varphi = 0.65$ (least stable flame). The average images provide a source of data on mean flame structure that can be compared directly to code predictions. These OH image for the HS, $\varphi = 0.80$ case show that the highest concentrations of OH in the

central recirculation zone directly above the injector. This suggests that the recirculation of these combustion intermediates back into the ignition zone is an important factor in stabilizing this flame. The highest OH concentrations for the MS, φ = 0.65 case (albeit at a much lower concentration) show in the central recirculation zone directly above the injector and also in the side recirculation zones. This suggests that at lower swirl and fuel equivalence ratio the side recirculation zones have a significant role in flame stabilization. This is consistent with observations drawn by Murray (1998) from the LDA velocity measurements.

Examples of OH PDF distributions for the HS, φ = 0.80 case are presented in Figure 6. The distributions are based on the count distributions obtained at the location of each of the selected pixel sites as illustrated on the companion map of the mean image. The peak and average counts for each selected location are included on each of the PDF distributions. The average counts range from 181 (Location a) to 1652 (Location g). The peak counts range from 600 (Location a) to 4633 (Location g). It is evident that the distributions are not Gaussian (a common modeling assumption) but may be better described by a beta distribution. The shape, count level, and PDF distribution are all useful when comparing to model predictions.

LDA GAS VELOCITY MEASUREMENTS

An important part of this ATS study has been the mapping of velocity profiles for the premixed natural gas/air burner. These velocity measurements were made using a conventional two-color four-beam Laser Doppler Anemometer (LDA) system in forward-scatter mode. This LDA configuration allows the simultaneous measurement of either axial and tangential or axial and radial velocity components. The details of the LDA instrument have been provided elsewhere (Hedman, et al., 1998; Murray, 1998)

Due to the nature of LDA data acquisition, the data contains a distribution of velocity measurements for each measurement location. These velocity distributions were used to determine: 1) mean (u, v, w) and standard deviation velocities (u', v', w'), 2) Reynolds stresses (u'v' and u'w'), and 3) the probability density function (PDF) at multiple locations in the flame. The local flow characteristics at multiple locations throughout the burner have allowed creation of iso-contour maps of the flow characteristics in the burner flame that was optically accessible. Optical access allowed most of the interesting flame zones to be characterized.

The velocity data yield considerable insight into the flow structure inside the burner flame. This information coupled with coherent anti-Stokes Raman spectroscopy (CARS) temperature and species data and planar laser induced florescence (PLIF) data give insights of the reaction mechanisms and flame structures in the premixed natural gas/air flame used for this study. In addition, the data have been used as a benchmark for combustion modeling testing and evaluation.

Complete data sets (complete radial profiles at a greater number of axial locations) were obtained for the medium swirl, and high swirl injectors at φ = 0.65 and φ = 0.80. Consequently, four complementary sets of instantaneous axial & radial velocities, and axial & tangential velocities have been obtained for the premixed, natural gas combustor at fuel equivalence ratios of 0.65 and 0.80 for both the medium (SN = 0.74) and high (SN = 1.29) swirl burners. The two component velocity data (either axial & radial, or axial & tangential) were collected at approximately 130 separate radial/axial in situ locations and 200 in situ axial/tangential locations within the flame zone. Four thousand instantaneous data points were collected at each location. Each data set provides mean and standard deviation axial, radial, and tangential velocity data, as well as two component Reynolds stress based on axial/radial and axial/tangential data sets. Axial, radial, and tangential probability density function distributions are also available for each test conditions and in situ location where data were collected. Only example results are presented in this paper. Complete results are available in Murray (1998) and Hedman, et al. (1998).

Data sets were taken at axial locations of 10, 20, 30, 40, 50, 75, 100, 125, 150, 200, and 250 mm above the base of the combustor. The basic flow field in the combustor was illustrated using interpolated iso-contours of the mean and standard deviation of each component of velocity (axial, radial, and tangential), and Reynolds stress. The PDFs provided insight into the turbulent characteristics throughout the combustor, and across the shear zones within the flame structure.

Example results from the LDA velocity measurements are presented in Figure 7 for the mean axial iso-velocity data. As with the PLIF images, the example contour plots are limited to the HS, φ = 0.80 (most stable) case and the MS, φ = 0.65 (least stable) case. The contours on the left side of each figure were generated by duplicating the data from the right side of each figure. Limited data were obtained at the negative locations near the centerline (-6 mm, and -3 mm). The negative locations were included in the test matrix to determine the degree of symmetry in the results. Generally, the velocity fields were very symmetric about the centerline. The combined images were superimposed on a schematic of the combustor to provide a spatial reference frame for the flow field.

The visual flame at the HS operating condition, Figure 7(A) was well attached, with the base of the funnel cloud created by the vortex structure being drawn into the nozzle and out of sight. The sharp axial velocity peak near the injector exit is readily apparent, as well as the high velocity regions that border the central recirculation vortex created by the swirling flow. The axial velocity decays rapidly above the injector due in part to dissipation in the shear layer and the stagnating effects of the combustion reaction. That the flow is dominated by recirculation zones is clearly evident in the channel-like regions of positive axial velocity being bordered by zero velocity contours. The splitting of the flows along the walls into portions of upward and downward moving gas is confirmed by the contours located between the large central recirculation zone and the smaller outside recirculation zone. It can be seen that the axial velocity is highest at the midpoint between the recirculation zones and then decays outward in both directions as part of the flow moves upward and the other part is drawn down into the region of negative axial velocity near the wall.

Similar observations about the flow structures can be drawn from the axial velocity contour plot for the medium swirl injector, Figure 7(B). The flow patterns are very similar, but the flame structure is somewhat broader, and the velocities in the recirculation zones are of a somewhat lower magnitude. The visible flame with the MS injector did not enter the injector like the HS flame was observed to do.

Multiple (ca 4000) velocity measurements (axial, radial, and tangential) at many in situ locations (ca 200) in a flame zone allow local PDF information throughout the flame structure to be determined. The measured PDF information provides considerable insight into the turbulent characteristics of flow, and provides, as does the mean and standard deviation velocity data, important results needed for model development and validation.

Figure 8 presents some example axial velocity PDFs generated from the LDA data at $\varphi = 0.80$ for the HS burner. The PDFs presented in this figure were calculated from about 4000 axial velocity measurements taken at an axial location of 80 mm above the injector and at radial locations of 2, 8, 14, 20, 26, 32, 38, and 44 mm from the burner centerline. These results provide PDFs from the central recirculation zone (negative mean velocities) through the shear layer into the zone of positive axial flow. At this axial location, the axial velocity distribution was nearly Gaussian near the centerline (negative flow velocity). But as one moves from inside the vortex, through the shear zone and into the surrounding outside gases, the distribution begins to become distorted, reflecting the flow structure outside the shear region. In fact, the distribution becomes bimodal as the LDA diagnostic volume straddles the shear zone (v = 0 m/s). As one moves past the shear zone, the distribution once again begins to show a more Gaussian distribution in the positive axial flow that exists in this region. At a position lower in the combustor, the shear layer was much thinner, and the transition through the shear layer would first favor the negative velocity side then the positive side. The bi-modal PDF distributions show characteristics of both sides of the shear layer.

CARS TEMPERATURE MEASUREMENTS IN THE LSGTC

Coherent anti-Stokes Raman Spectroscopy (CARS) is an advanced laser-based diagnostic technique that allows in situ measurement of gas temperature and selected species concentrations. The CARS instrument at this laboratory has been used in several previous studies to obtain spectral data for the N_2, O_2, CO, and CO_2 species in different flames (Boyack and Hedman 1990; Dawson and Hedman, 1996, Flores, 2001). The CARS technique utilizes the Raman shift that results when a particular gas molecule is energized by a high power laser. The Raman shift is attributed to the inelastic scattering that occurs between the photons of the laser beam and the orbiting electrons of the molecule. With the inelastic scattering, energy can be exchanged in either direction between the photons and electrons. This results in a spectral signature that is quantum shifted either up or down from the pump laser frequency. These spectra, which contain information about temperature and species concentration, are referred to as the Stokes or anti-Stokes signals. Comparison of the measured spectra with computed spectra from quantum theories (Farrow, 1995) allows the gas temperature and/or species concentration to be determined.

The Raman signal is relatively very weak, and is scattered in 4π steradians. Thus, Raman scattering is limited in signal strength. CARS utilizes the Raman effect but combines a laser beam tuned to the Stokes frequency of a particular molecule with two laser beams at the pump frequency. This nonlinear wave mixing process is illustrated in Figure 9 for temperature (based on nitrogen) and CO concentration. The nonlinear wave mixing, illustrated in the wave vector diagram, produces a laser like beam at the anti-Stokes frequency that contains the spectral information. This laser-like beam, which may be 1000 times stronger than a Raman signal, can be focused into a broad band spectrometer where the spectra can be obtained and stored for later computer analysis.

The ACERC/BYU CARS instrument has been used to collect temperature and species concentration data for

the LSGTC. As with the PLIF and LDA measurements, four test conditions [SN = 0.74 (MS) and 1.29 (HS) at fuel equivalence ratios (φ) of 0.65 and 0.80] were selected for this study. However, only example temperature results are included in this paper. As with the velocity measurements, the results are presented as iso-contour plots of gas temperature. Approximately 1000 separate instantaneous CARS measurements were made at various in situ locations within the combustor. As with the PLIF and LDA data, the results have been reduced in terms of mean temperature, standard deviation temperature, and temperature PDFs at selected locations within the combustor.

It is customary with velocity data to divide the standard deviation values by the local mean velocity to determine the local turbulent intensity. This was not possible with the velocity data reported above because of the recirculation zones bounded by zero velocity contours. Turbulent intensities based on these velocity measurements would produce regions where the turbulent intensity is indeterminate. However, this restriction does not apply to the CARS temperature results. Consequently, iso-contour plots of the normalized standard deviation in temperature ($\sqrt{T'T'}/\bar{T}$) provide useful insight into the regions of significant temperature changes.

As with PLIF and LDA results, example gas temperature contours and temperature turbulence contours for the HS, φ = 0.80 (most stable) case, and MS, φ = 0.65 (least stable) case are presented in Figure 10. The iso-contour maps were created from multiple instantaneous measurements at about 200 separate in situ locations within the flame zone. The differences between the most stable case and the least stable case are striking. The differences between peak (1636 K and 1472 K) and minimum (402 K and 323 K) temperatures for the two cases are thought to be primarily a result of the different fuel equivalence ratios. The differences between normalized standard deviations in temperature (60% versus 39%, and 5.5% versus 4.4%) are thought to be caused by a combination of the different fuel equivalence ratios and swirl numbers. The difference in flame structure between the two cases is reflected in the contour plots of both the mean and normalized standard deviation in temperature. The contour plots show that the highest mean temperature and standard deviations for the HS case (most stable) are much closer to the burner inlet, which suggests a stronger vortex structure and a more stable flame in this case. This is consistent with the LDA velocity results and the OH PLIF results presented above.

The ability to collect multiple instantaneous ***in situ*** data at many locations within the flame zone of a practical combustor allows the PDF distributions to be obtained throughout the flame zone. These PDF distributions are of interest to code developers and are useful in characterizing turbulence models, and in verifying code predictions. Example OH PLIF PDFs and axial velocity PDFs were earlier in the paper for the HS, φ = 0.80 case. Figure 11 presents example temperature PDFs for this same case at the locations indicated on the companion mean temperature contour plot. The PDF data show a wide range, which tends to confirm high levels of turbulence as seen in the velocity PDF data, and in the visual images shown in the PLIF data. The shape of the temperature PDFs are not quite Gaussian in most locations in the flame, but like the velocity data shown in Figure 8, show a bimodal distribution in regions that straddle the shear zone between the inner and outer recirculation zones.

SUMMARY AND CONCLUSIONS

A laboratory-scale gas turbine combustor (LSGTC) and associated laser-based diagnostic instruments were used to make in situ combustion measurements in a lean premixed natural gas flame that closely simulates flames that would exist in a utility gas turbine engine. Use of advanced optical diagnostics permitted near-instantaneous, non-intrusive measurement of velocity (LDA), temperature (CARS), and instantaneous flame shape (PLIF of OH) that are essential for model validation.

Four separate experimental test conditions were examined during the course of this study. Complete data sets from measurements of PLIF, LDA, and CARS were obtained at medium and high swirl levels for two lean premixed natural gas stoichiometric ratios (φ = 0.65 and φ = 0.80). The high swirl case at φ = 0.80 was the most stable flame condition tested. The medium swirl case at φ = 0.65 was very near the lean flammability limit for this burner, and was very unstable.

The stochastic nature of the flame is readily apparent from the PLIF images presented. The OH images flames at high swirl show increased stability and more intense OH images at both high and low fuel equivalence ratios. The images at medium swirl and φ = 0.80 are also intense and stable. The flame at medium swirl and φ = 0.65 was very unstable.

The OH PLIF image for the HS, φ = 0.80 case shows the highest concentrations of OH in the central recirculation zone directly above the injector. This suggests that the recirculation of these combustion intermediates back into the ignition zone is an important factor in stabilizing this flame. The highest OH concentrations for the MS, φ = 0.65 case show in the central recirculation zone directly above the injector and also in the side recirculation zones. This suggests that at lower swirl and fuel equivalence ratio the side

recirculation zones have a significant role in flame stabilization.

Examples of PDF distributions for the HS, φ = 0.80 case were presented. The OH PLIF distributions are not Gaussian (a common modeling assumption) but may be better described by a beta distribution.

Velocity measurements were made using a conventional two-color four-beam Laser Doppler Anemometer (LDA) system in forward-scatter mode. The visual flame at the HS operating condition was well attached with the base of the funnel cloud created by the vortex structure being drawn into the nozzle and out of sight. A sharp axial velocity peak existed near the injector exit. High velocity regions also bordered the central recirculation vortex created by the swirling flow. The axial velocity decays rapidly above the injector due in part to dissipation in the shear layer and the stagnating effects of the combustion reaction. The flow is dominated by recirculation in the channel-like regions of positive axial velocity bordered by zero velocity contours. The flows split along the walls into portions of upward and downward moving gas. The axial velocity is highest at the midpoint between the recirculation zones and then decays outward in both directions as part of the flow moves upward and the other part is drawn down into the region of negative axial velocity near the wall.

The measured velocity PDF information provides considerable insight into the turbulent characteristics of the flow. The axial velocity PDF distribution was nearly Gaussian near the centerline (negative flow velocity). However, the distribution became distorted near the shear region. The PDF distribution becomes bimodal as the LDA diagnostic volume straddles the shear zone (v = 0 m/s). As one moves past the shear zone, the distribution once again begins to show a more Gaussian distribution in the positive axial flow that exists in this region. The bimodal PDF distributions show characteristics of both sides of the shear layer.

The CARS instrument was used to collect temperature and species concentration data for the LSGTC. The standard deviations of the gas temperature normalized by the local mean gas temperatures were used to determine principal reaction zones. The differences between peak temperature (1636 K and 1472 K) and minimum temperature (402 K and 323 K) for the two cases is thought to be primarily a result of the different fuel equivalence ratios. The differences between normalized standard deviations in temperature of 60% versus 39%, and minimum temperature turbulence levels of 5.5% versus 4.4%, are thought to be caused by a combination of the different fuel equivalence ratios and swirl numbers. The temperature contours for the HS case (most stable) are much closer to the burner inlet, which suggests a stronger vortex structure and a more stable flame in this case. This is consistent with the LDA velocity results and the OH PLIF results.

The temperature PDF data confirms high levels of turbulence as seen in the velocity PDF data, and in the visual images shown in the PLIF data. The shape of the temperature PDFs are nearly Gaussian in most locations in the flame, but show a bimodal distribution in regions that straddle the shear zone between the inner and outer recirculation zones.

ACKNOWLEDGEMENTS

This study was supported by the DOE/METCCooperative Agreement No. DE-FC21-92MC29061 through Subcontract No. 93-01-SR014 with SCERDC (Dr. Daniel P. Fant, and Dr. Lawrence P. Golan, Project Directors). Students contributing to the experimental measurements included Jason Haslam, Robert Dawson, Robert Murray, Stewart Graham, Wayne Timothy, and Daniel Flores. Additional support from ACERC, and BYU is acknowledged.

REFERENCES

Beer, J. M., and Chigier, N. ***Combustion Aerodynamics***, Applied Science Publishers, London (1972).

Boyack, K. W., and Hedman, P.O., "Dual-Stokes CARS System for Simultaneous Measurement of Temperature and Multiple Species in Turbulent Flames," Twenty-Third Symposium (International) on Combustion, The Combustion Institute, Pittsburgh, PA (1990).

Dawson, R. W. and Hedman. P.O., “A Technique for Determining Instantaneous N_2, CO, O_2, CO_2, and H_2O Species Concentrations Using Multiplex CARS in Premixed Gaseous Flames,” presented at the Western States Section/Combustion Institute, Paper No. 96F-087, The University of Southern California, Los Angeles, California (October 28-29, 1996).

Farrow, R. L., Personal Communication: CARSFT Computer Code for Calculating Coherent Anti-Stokes Raman Spectra, Sandia National Laboratories, Livermore, California (1995).

Flores, D. V., “A Study of Premixed Natural Gas-Air Combustion Based on CARS and LDA Measurements on a Laboratory-Scale Gas Turbine Combustor,” Ph.D. Dissertation, Chemical Engineering Department, Brigham Young University, Provo, Utah 84602 (In Preparation 2001).

Gupta, A. K., Lilley, D. G. and Syred, N. Swirl Flows, Abacus Press (1984).

Hedman, P. O., Sturgess, G. J., Warren, D. L., Goss, L. P., and Shouse, D. T., "Observations of Flame Behavior from a Practical Fuel Injector Using Gaseous Fuel in a Technology Combustor," Journal

of Engineering for Gas Turbines and Power, Vol. 117, pp 441-452 (July 1995).
Hedman, P. O., and Warren, D. L., "Turbulent Velocity and Temperature Measurements from a Gas-Fueled Technology Combustor with a Practical Fuel Injector," Combustion and Flame, Vol. 100, pp 185-192 (1995).
Hedman, P. O, Smoot, L. D., Brewster, B. S. and Fletcher, T. H., "Final Report-Combustion Modeling in Advanced Gas Turbine Systems," Advanced Combustion Engineering Research Center, Brigham Young University, Provo, Utah 84602, U.S. Department of Energy, Morgantown Energy Technology Center, Cooperative Agreement No. DE-FC21-92MC29061, Subcontract No. 93-01-SR014, Clemson University Research Foundation South Carolina Energy Research and Development Center, Clemson, South Carolina 29634-5702 (February 28, 1998).
Murray, R. L., "Laser Doppler Anemometry Measurements in a Turbulent, Premixed Natural Gas/Air Combustor," M.S. Thesis, Chemical Engineering Department, Brigham Young University, Provo, Utah 84602 (April 1998).
Roquemore, W. M., Personal Communication, Wright-Patterson Air Force Base, Dayton, Ohio (1992).
Sturgess, G. J., Sloan, D. G., Lesmerises, A. L., Henneghan, S.P., and Ballal, D.R., "Design and Development of a Research Combustor for Lean Blowout Studies", ASME Journal of Engineering for Gas Turbines and Power, Vol. 114, pp 13-19 (1992) 35th International Gas Turbine and Aeroengine Congress and Exposition, Brussels, Belgium (June 1990).
Warren, D. L., and Hedman, P. O., "Differential Mass and Energy Balances in the Flame Zone from a Practical Fuel Injector in a Technology Combustor," Journal of Engineering for Gas Turbines and Power, Vol. 119, pp 352-361 (April 1997).

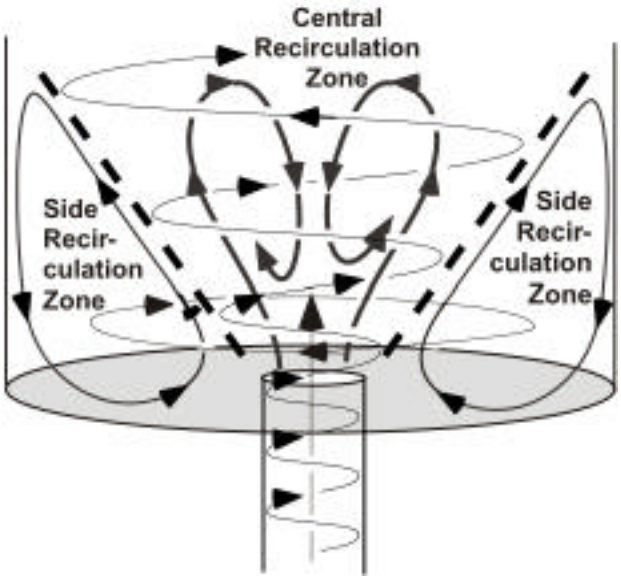

Figure 1. Flow patterns in a confined, bluff-base, premixed, swirl-stabilized combustor (adapted from Gupta, et al., 1984).

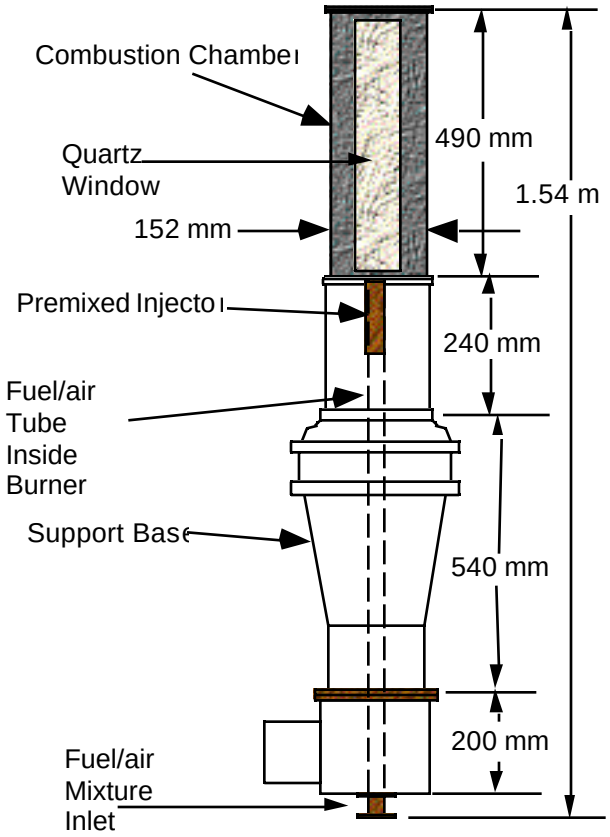

Figure 2. Schematic of premixed combustor (adapted from Schmidt and Hedman, 1995).

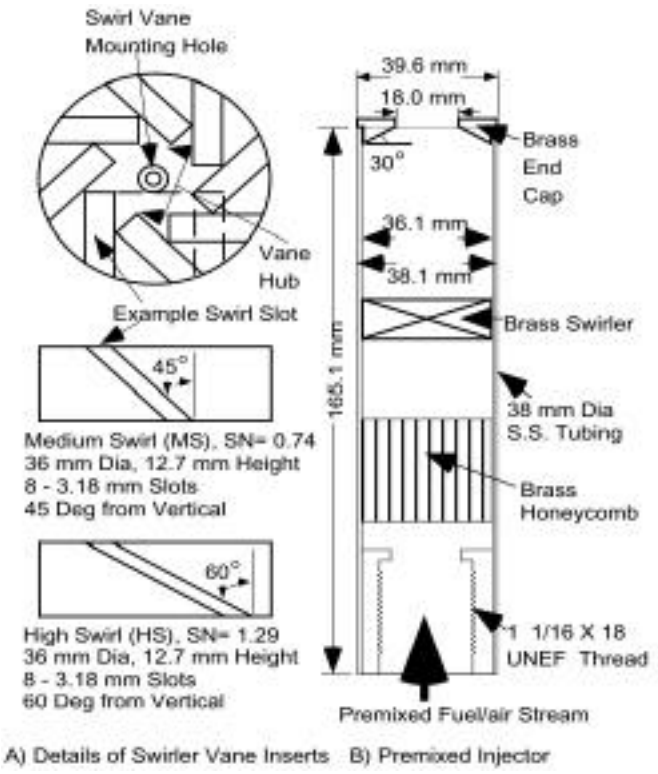

Figure 3. Schematic of premixed injector and the medium and high swirl block inserts (adapted from Schmidt and Hedman, 1995).

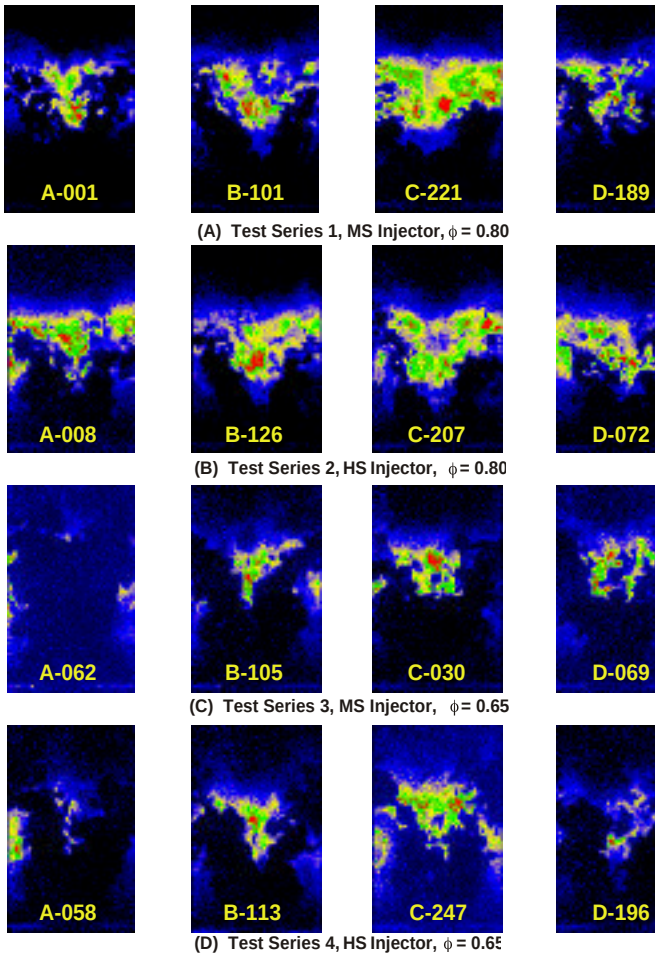

Figure 4. Example instantaneous OH PLIF images at each test condition. A: near minimum image; B: near average image; C: near maximum image; D: image with odd structure.

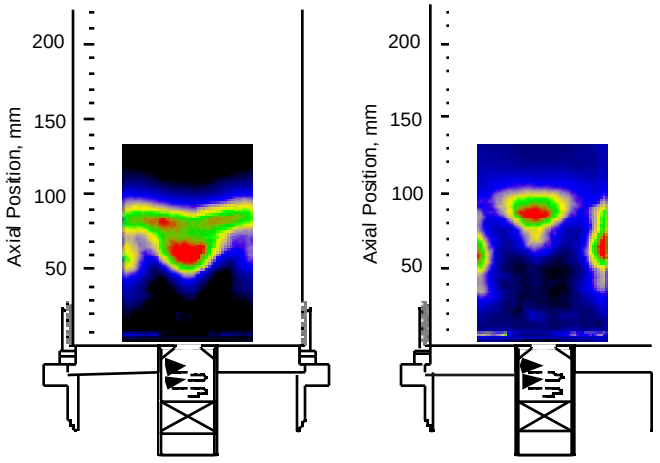

Figure 5. Example of mean PLIF images of OH in the ATS burner (premixed natural gas/air, air flow = 500 slpm). Left: high swirl, φ = 0.80; Right: medium swirl, φ = 0.65.

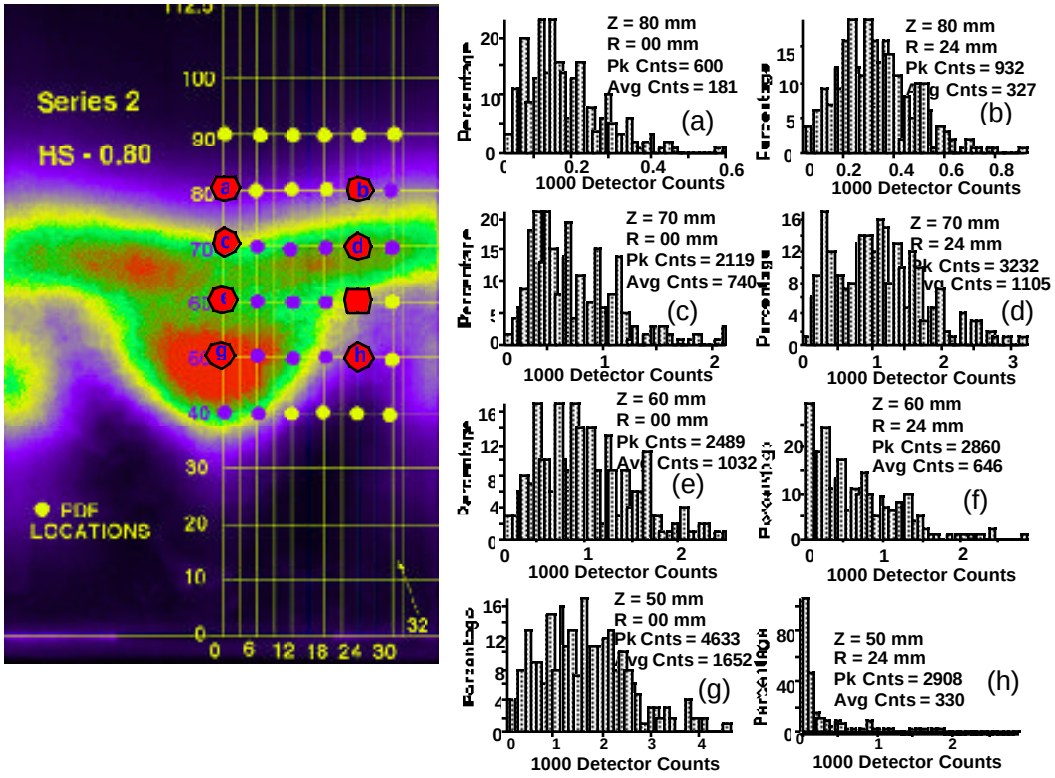

Figure 6. Example PDFs from OH-PLIF images for the high swirl, φ = 0.80 case.

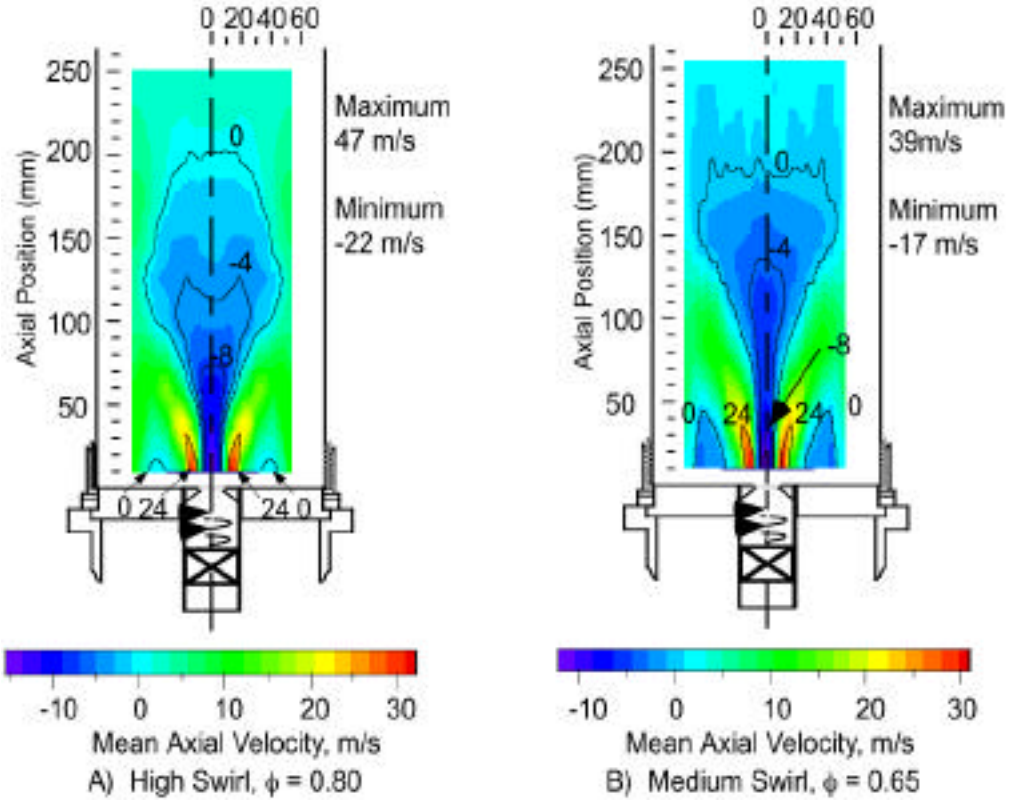

Figure 7. Example mean iso-axial velocity contours from combined axial/tangential data sets.

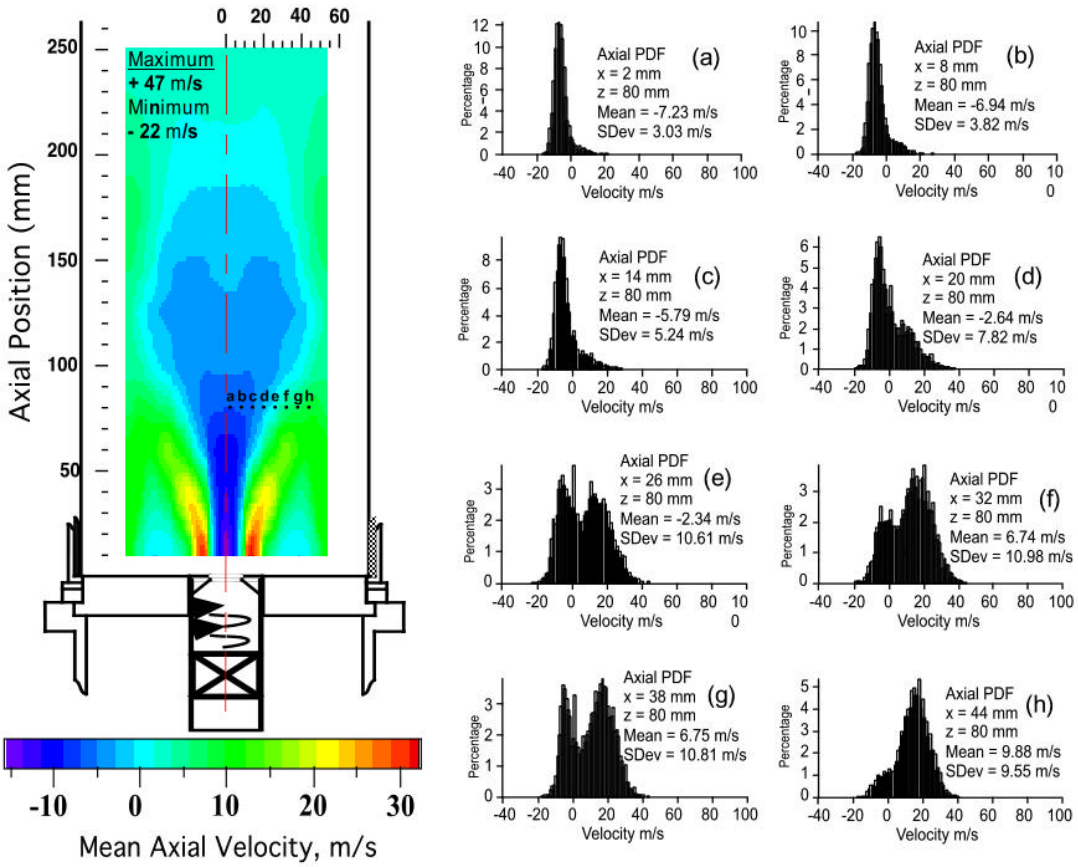

Figure 8. Example of axial velocity PDF's across flame shear layer for the high swirl, φ = 0.80 case.

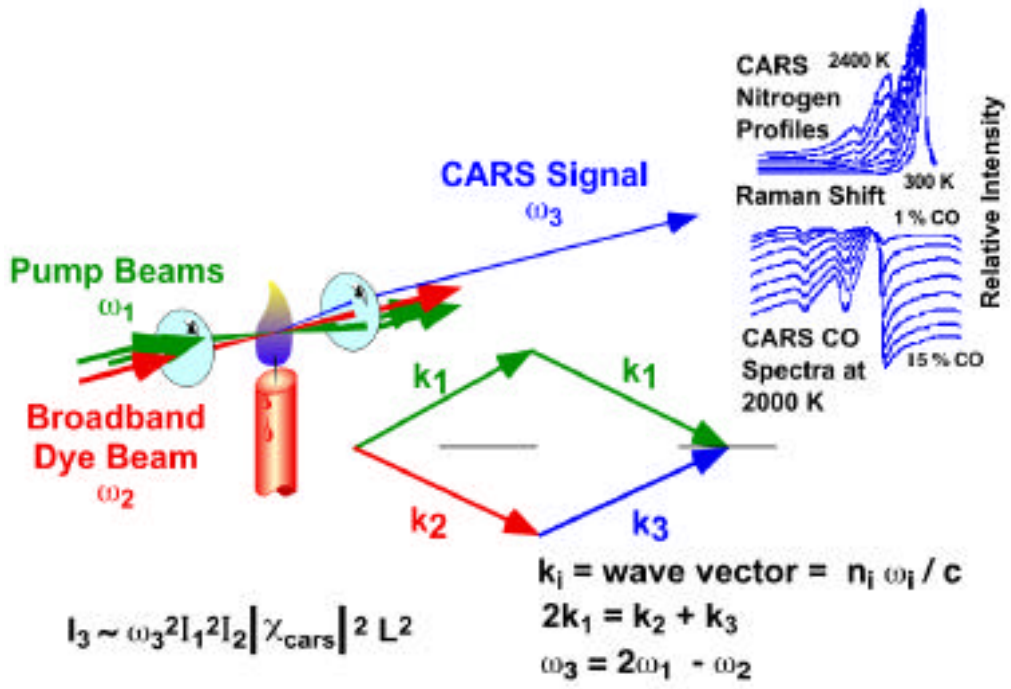

Figure 9. Details of CARS Spectroscopy.

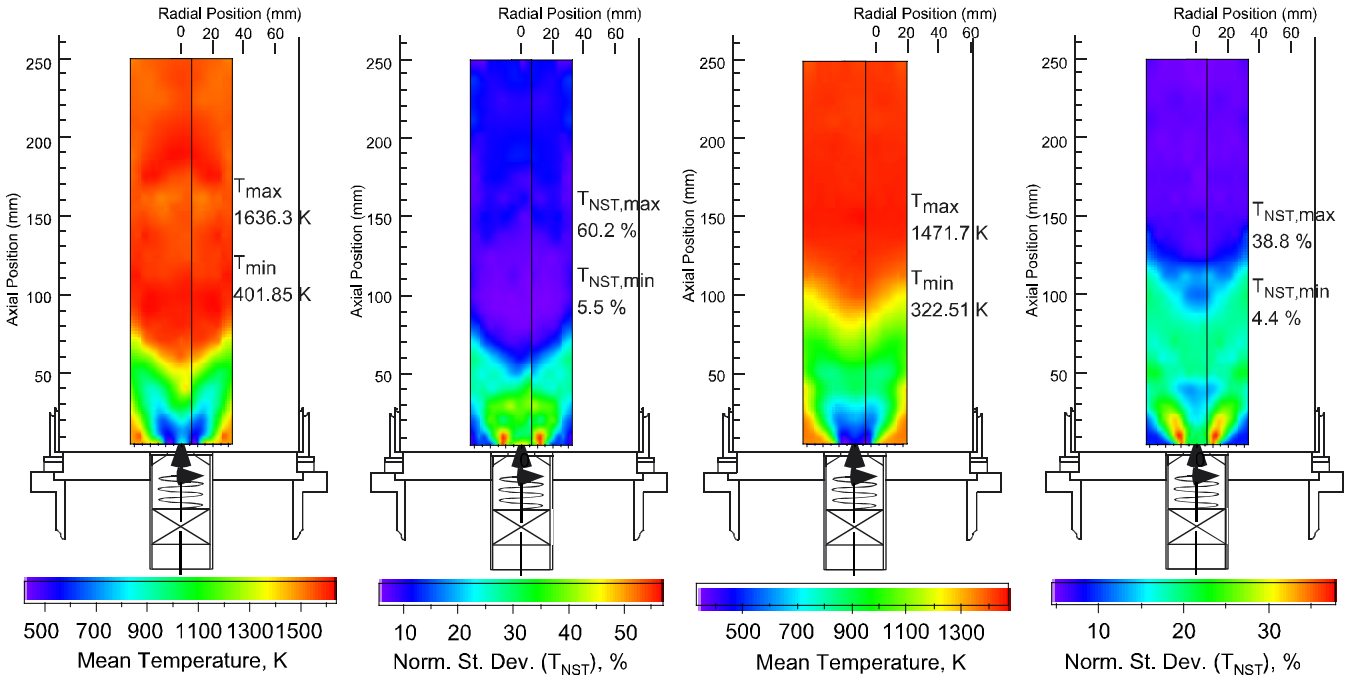

A) High Swirl, ϕ = 0.80, 500 slpm Air Flow Rate B) Medium Swirl, ϕ = 0.65, 500 slpm Air Flow Rate)

Figure 10. Iso-Contours of Mean Temperature and Normalized Standard Deviation Based on Instantaneous CARS Temperature Measurements

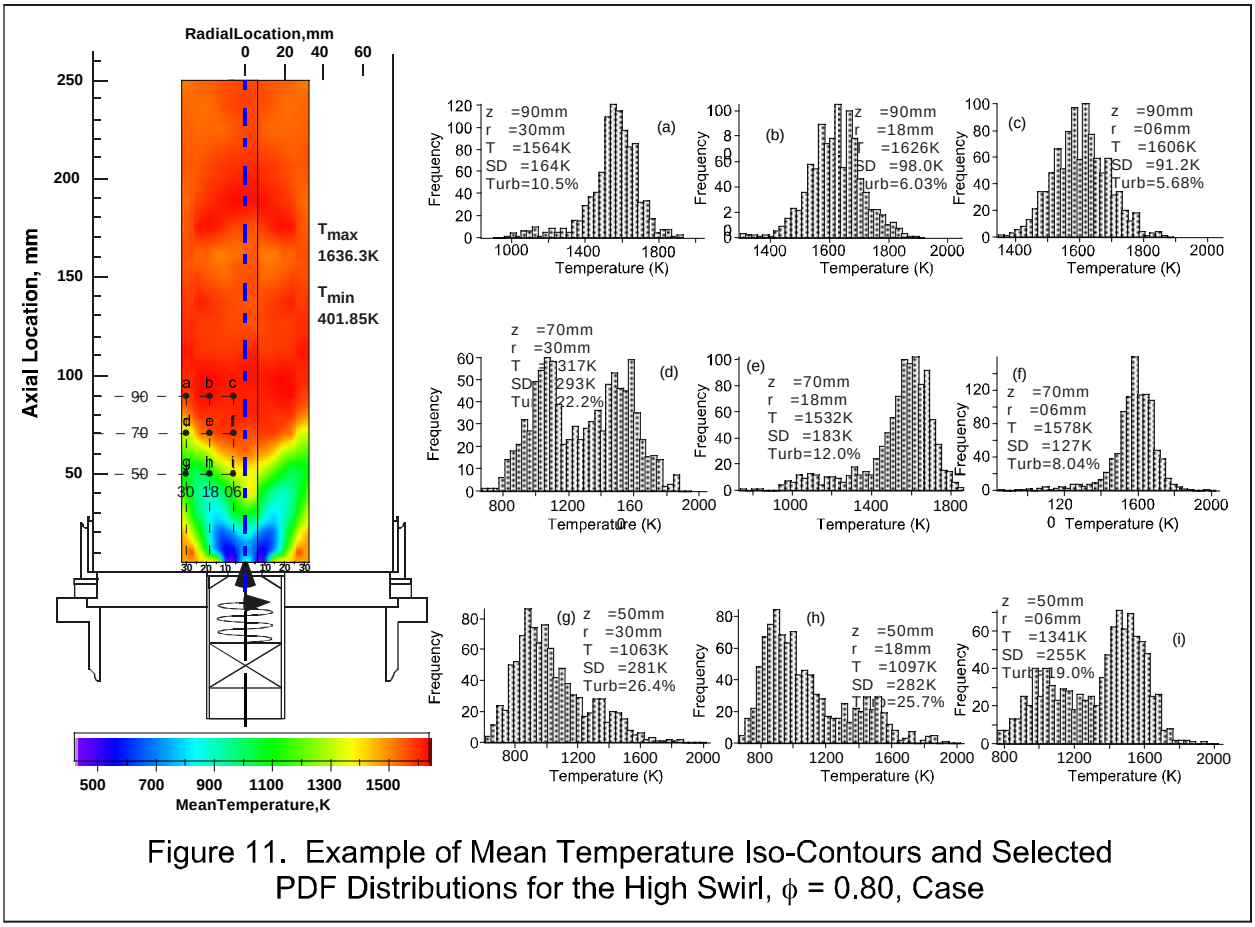

Figure 11. Example of Mean Temperature Iso-Contours and Selected PDF Distributions for the High Swirl, ϕ = 0.80, Case